Hindawi Publishing Corporation
Journal of Nanomaterials
Volume 2012, Article ID 454507, 7 pages
doi:10.1155/2012/454507

Research Article

Fabrication of Photofunctional Nanoporous Membrane and Its Photoinactivation Effect of Vesicular Stomatitis Virus

Kang-Kyun Wang,[1] Bong-Jin Kim,[1] Si-Hwan Ko,[2] Dong Hoon Choi,[3] and Yong-Rok Kim[1]

[1] *Department of Chemistry, Yonsei University, Shinchon-Dong 134, Seodaemun-Gu, Seoul 120 749, Republic of Korea*
[2] *Department of Microbiology, College of Medicine, Yonsei University, Seoul 120 752, Republic of Korea*
[3] *Cardiology Division, Cardiovascular Center, College of Medicine, Yonsei University, Seoul 120 752, Republic of Korea*

Correspondence should be addressed to Yong-Rok Kim, yrkim@yonsei.ac.kr

Received 29 May 2011; Accepted 11 July 2011

Academic Editor: Amir Kajbafvala

Fabrication and photophysical study of photofunctional nanoporous alumina membrane (PNAM) were performed, and its application of photodynamic antimicrobial chemotherapy (PACT) was investigated. Nanoporous alumina membrane (NAM) was fabricated by two-step aluminium anodic oxidation process. Surface of the fabricated NAM was modified with organo-silane agent to induce covalent bonding between NAM and a photosensitizer (PtCP: [5,10,15-triphenyl-20-(4-methoxycarbonylphenyl)-porphyrin] platinum). PtCP was covalently bonded to the surface of the modified NAM by nucleophilic acyl substitution reaction process. The morphology and the photophysical properties of the fabricated PNAM were confirmed with field emission scanning electron microscope (FE-SEM), steady-state spectroscopies, and nanosecond laser-induced time-resolved spectroscopy. For the efficacy study of PNAM in PACT, an enveloped animal virus, vesicular stomatitis virus (VSV), was utilized as a target organism. Antiviral effect of the PNAM-PACT was measured by the extent of suppression of plaque-forming units (PFU) after the light irradiation. In the cultures inoculated with PACT-treated VSV, the suppression of PFU was prominent, which demonstrates that PNAM is a potential bio clean-up tool.

1. Introduction

Reactive oxygen species (ROS) have been a subject of the extensive studies due to their broad applications such as photodynamic therapy (PDT), photovoltaic device, light harvest coating, and photocatalyst [1, 2]. Recently, the application area of ROS has been expanded into elimination of environmental pollutants such as toxic chemicals, endocrine disruptors, virus, and bacteria [3, 4]. The environmental applications require the high efficiency of ROS generation along with repeatability, the prevention of secondary contamination, and the easy recycling. In order to meet some of these factors, ROS generation of mesoporous materials has been demonstrated with zeolite and MCM-41 functionalized with photosensitizers [5]. By the fixation of photosensitizers onto zeolite or MCM-41, thermal stability and handling advantage could be achieved. However, both porous materials have a powder like property and a few nanometers of very small pore diameter which disturbs the good contact between the ROS and the target systems [6]. However, the nanoporous membranes can provide the good contacts between the ROS and the target, and the easy handling advantage and recycling together due to their advantages of pore diameter control, unidirectional ordered pore direction, and free-standing nature of membrane.

In this work, we report a fabrication of the photofunctional nanoporous alumina membrane (PNAM) and its photophysical property. The nanoporous alumina membranes were fabricated by two-step aluminum anodic oxidation process [7]. The inner and the outer surfaces of the fabricated NAMs were modified with organo-silane agent [8–11]. The photosensitizer (PtCP: [5,10,15-triphenyl-20-(4-methoxycarbonylphenyl)-porphyrin] platinum) was covalently bonded to the amine-terminated NAM surface by a nucleophilic acyl substitution reaction [12]. The singlet oxygen, an active component of the ROS generated from the

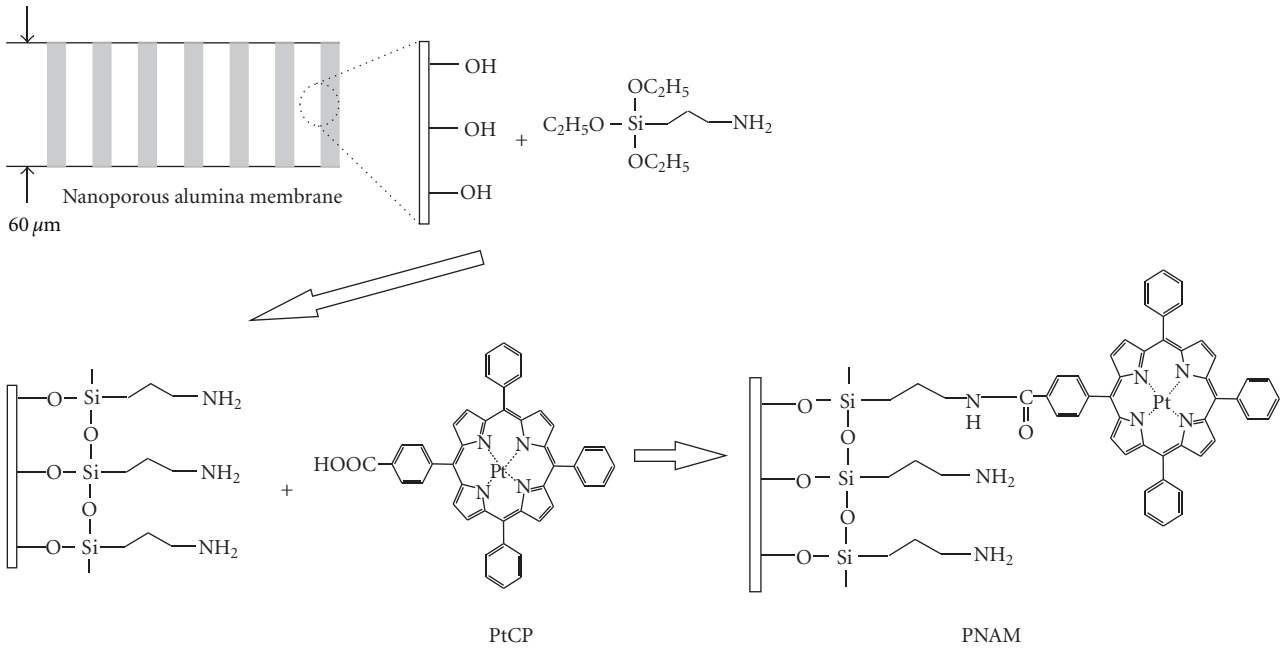

Scheme 1: Preparation of photofunctional nanoporous alumina membrane.

fabricated PNAM, was directly monitored with laser-induced time-resolved spectroscopic method. To open the possibility for its environmental application, PNAM was applied for the removal of a virus without rendering cytotoxicity to the cells *in vitro*. It resulted in the complete suppression of plaque forming ability of vesicular stomatitis virus (VSV) by PNAM-mediated PACT (photodynamic antimicrobial chemotherapy).

2. Experiment

2.1. Materials. The fabrication procedure of the PNAM is shown in Scheme 1. Preparation details of the photosensitizer (PtCP: [5,10,15-Triphenyl-20-(4-methoxycarbonylphenyl)-porphyrin] platinum) and the nanoporous alumina membrane (NAM) were reported in the references [7, 13]. All solvents were purchased from Aldrich and used without further purification. For the surface modification of NAM, NAM was immersed into the APTES ((aminopropyl)triethoxysilane, 0.1 M)/$CHCl_3$ solution at room temperature for 1 h [8–11]. After washing and drying, the surface-modified NAM was immersed in PtCP (10^{-5} M)/toluene at 50°C for 24 h and then washed with pure toluene and distilled water.

2.2. Methods

2.2.1. Spectroscopic Measurements. Surface morphologies of NAMs were observed by a field emission scanning electron microscopy (FESEM, JEOL, 6500F). Surfaces of the modified NAM and the fabricated PNAM were confirmed by ATR-IR spectra with a ATR-IR spectrophotometer (Nicolet, impact 400). Steady-state absorption and luminescence spectra were obtained by using a UV-Vis spectrophotometer (Hitachi, U-2800) and a spectrofluorimeter (Hitachi, F-4500), respectively. For the membrane sample, the diffuse reflectance spectra were recorded by a UV-Vis spectrophotometer (Jasco, V-550) equipped with an integrating sphere (Jasco, ISV-469). The Nd-YAG-pumped OPO laser (BMI, OP-901, 10 Hz, 5 ns FWHM pulse) was utilized as an excitation source for the detection of time-resolved singlet oxygen phosphorescence. The phosphorescence signal was collected at the perpendicular angle to the excitation beam and detected with a monochromator (Optometrics LLC, mini-chrom04) and NIR-PMT (Hamamatsu, H9170-45). The signal was acquired by 500 MHz digital oscilloscope and transferred to a computer for further analysis [13, 14].

2.2.2. Biological Activity

General. The established cell lines of A549, Vero, and vesicular stomatitis virus (VSV, Indiana serotype) were originally purchased from ATCC (Rockford, Md, USA) and have been maintained at −70°C and 1 atm. For the evaluation of the efficacy with PNAM-mediated PACT on viral inactivation, A549 cells were used throughout the experiments. For viral preparation, VSV was propagated in Vero cells. Both the cell lines were maintained in Eagle's minimal essential medium (MEM) supplemented with 10% fetal bovine serum (both supplied by Gibco RBL, Grand Island, NY, USA), penicillin (100 units/mL), and streptomycin (100 μg/mL). The viral suspension free from the host cell debris was ultracentrifuged at 100,000 g for 2 h at 4°C (Beckman, Calif, USA). After centrifuging, protein content of the VSV pellet was determined by using the Bio-Rad protein assay (Bio-Rad Laboratories, Alfred Nobel Drive, Hercules, Calif, USA). The A549 cell grown in MEM was used as a host cell

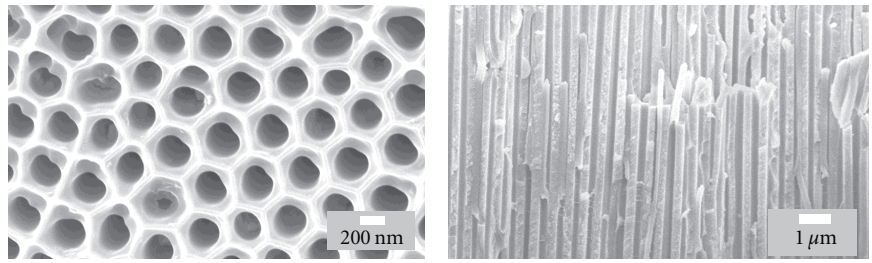

(a) (b)

Figure 1: FE-SEM images of (a) the top surface view of nanoporous alumina membrane with the pore diameter of 250 nm and (b) its cross-section view.

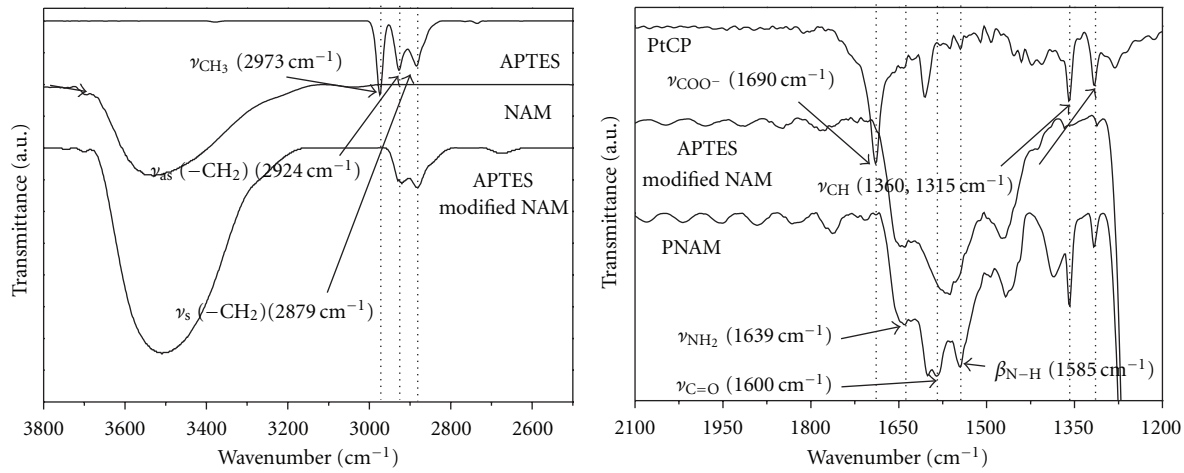

(a) (b)

Figure 2: ATR-IR spectra of (a) pure NAM, pure APTES, and the surface modified NAM with APTES, (b) pure PtCP, pure PNAM, and the surface modified NAM with APTES.

for various assays. The light source for irradiation was a nanosecond Nd-YAG-pumped OPO laser (BMI, OP-901, 10 Hz, 5 ns FWHM pulse). The total power output for the irradiation was measured with a laser power meter (Ophir opironics Ltd., Nova, Israel). Virus in suspension (1 mL in a 1 × 1 quartz cell) was treated by PNAM irradiated with 5mWof light for 1 hr. The virus solution treated with photo-irradiated PNAM was kept in dark in order to protect the samples from ambient light exposure. All experiments were performed under the light-controlled condition in a biosafety box.

Plaque-Forming Assay. For a plaque-forming assay, A549 cells were seeded (2×10^5) in 6-well tissue culture plates in the growth media and allowed to form a confluent monolayer. All viruses that were treated with light only, PNAM only, and the irradiated PNAM in 1 mL of the solutions were inoculated into the cells and allowed to attach to the cells by rocking randomly for 1 h at 37°C under 5% CO_2 humidified atmosphere. For a negative control, the cells treated with a phosphate-buffered saline (PBS) were used to assure the viability of the cells. The culture fluid was removed by aspiration and washed twice with MEM. Each well was overlaid with 2 mL of a mixture of 2% agarose and 2 × MEM (1 : 1) and then incubated for 48 h at 37°C under 5% CO_2-humidified atmosphere. Thereafter, the cells were rinsed by PBS and fixed in 2% paraformaldehyde for 15 min. These were then rinsed twice with PBS for staining with crystal violet. The titers of virus were estimated by use of the plaque-forming assay [15]. Statistical evaluation was done by using the Mann-Whitney U test. Results were presented as the means ± the standard errors of the means (SEMs).

3. Results and Discussion

SEM images of the fabricated pure NAM are shown in Figure 1. The pore diameter of nanochannels is controlled to be 250 nm by the electrolyte solution of 0.3 M H_3PO_4 at the applied voltage of 40 V. Thickness of NAM is made to be 60 μm after the oxidation time of 10 hours. NAM is prepared as a free-standing film [7].

The surface modification of NAM with hydrophobic silane, APTES, and PtCP are confirmed with ATR-IR spectra. Figure 2(a) shows ATR-IR spectra of APTES, NAM, and the APTES-bounded NAM. The peaks of APTES in the spectrum are assigned to be the $-CH_3$ symmetric vibration

mode at 2973 cm^{-1}, the $-CH_2$ symmetric and asymmetric vibration modes at 2879 and 2924 cm^{-1}, respectively, from the references [8, 16]. The spectrum of NAM shows the $-OH$ stretching vibration modes at 3400 cm^{-1} [8, 9]. In the spectrum of the APTES bounded NAM, the peaks of the $-CH_2$ symmetric (2879 cm^{-1}) and asymmetric vibration modes (2924 cm^{-1}) remain same as the peaks of pure APTES. On the other hand, the $–CH_3$ (2973 cm^{-1}) vibration peak disappears significantly in its intensity. It is due to the removal step of the methyl group ($-CH_3$) of APTES during the attachment reaction process of APTES and NAM [11, 16, 17]. The increased peak intensity of the $-OH$ (3650 $\sim$3200 cm^{-1}) stretching vibration in Figure 2(a) implies that the hydroxyl group of the NAM surface is enhanced throughout the surface modification process. Therefore, the result confirms that the APTES is attached to the NAM surface by the silanisation reaction between the hydroxyl group of NAM and the ethoxy group of APTES. Figure 2(b) shows ATR-IR spectra of the surface modified NAM with APTES, PtCP, and the PtCP bounded surface modified NAM (PNAM). The peaks of PtCP in the spectrum are assigned to be the carbonyl stretching mode of the carboxyl group at 1690 cm^{-1}, the stretching vibration mode of the conjugated C=C bond at 1605 cm^{-1}, and the C–H stretching vibration mode at 1360, 1315 cm^{-1} from the references [18–20]. The spectrum of the surface modified NAM shows the stretching vibration mode of $-NH_2$ group at 1639 cm^{-1} [21, 22]. In the spectrum of the PtCP-bounded surface modified NAM, the peaks of the stretching vibration mode of C=C (1605 cm^{-1}), and the stretching vibration modes of C–H (1360, 1315 cm^{-1}) remain same. On the other hand, the carbonyl (1690 cm^{-1}) stretching mode peak disappears significantly in its intensity. And the C=O stretching mode and the N–H bending mode of new amide group are appeared at the 1600, 1585 cm^{-1}, respectively. It is due to the removal step of the carboxylic acid group ($-COOH$) of PtCP during the nucleophilic acyl substitution reaction process of PtCP and the surface modified NAM [12]. The appeared peaks of the C=O and the N–H (1600, 1585 cm^{-1}) stretching vibration imply that the amide group of the modified NAM surface is enhanced throughout the surface modification process. Therefore, IR data in Figure 2 confirms that PtCP is covalently bonded to the modified NAM surface by the nucleophilic acylation reaction between the carboxylic acid group of PtCP and the amine group of APTES [12].

Diffuse reflectance UV-Vis absorption spectrum of PNAM is presented in Figure 3(a) with the comparison of the absorption spectrum of the pure PtCP molecules in toluene. Absorption spectrum of the PtCP-bounded surface-modified NAM (PNAM) was obtained by using diffuse reflectance spectrophotometer to avoid the big scattering of the membrane. Diffuse reflectance spectrum is a type of the absorption spectrum measured by scattering from the surface of sample. This diffuse reflectance spectrum is translated into the absorption spectra by the Kubelka-Munk method [23]. The spectrum of PtCP shows one B band (400 nm) and two Q bands (510, 538 nm) [13]. The diffuse reflectance absorption spectrum of PNAM also includes the B and Q bands at the similar wavelengths but with the broader shape and the red-shifted peak position. Such difference in the peak width and position is possibly due to the self-coupling of the PtCP molecules attached on the surface and the inhomogeneous broadening nature of PtCP to the surface of PNAM [11, 24, 25]. The fluorescence was not observed for the pure PtCP and PNAM. Whereas the phosphorescence spectrum of PtCPin Figure 3(b), at 510 nm excitation, presents the peaks at 660 nm and 725 nm. In case of PNAM, the phosphorescence spectrum shows a similar red shift due to the same nature for the excited state of the PtCP molecules bonded to NAM as in their ground states [11].

The most critical factor for the proof of the singlet oxygen generation from PNAM is the direct detection of the phosphorescence from the singlet oxygen molecules generated by the photoexcited PNAM. The singlet oxygen phosphorescences of PtCP and the PtCP-bounded PNAM were measured at the detection wavelength of 1270 nm in air-saturated toluene and distilled aqueous solution. The measured phosphorescence signals are presented in Figure 4. The decays are fitted to a single exponential function, resulting in the lifetime of the singlet oxygen that depends on the environmental condition [14]. Singlet oxygen lifetime of the pure PtCP molecules in toluene solution is measured to be $\sim$29 μs (Figure 4(a)) that is a characteristic relaxation time of singlet oxygen in toluene solvent [13]. However, the singlet oxygen lifetime for PNAM with the pore diameter of 250 nm is 7.9 μs in toluene solution (Figure 4(b)). Assuming a typical diffusion coefficient for oxygen to be 2.69×10^{-9} m^2s^{-1} of D, the average distance that the singlet oxygen can diffuse in toluene is estimated to be approximately 394 nm during 29 μs of its lifetime from the root-mean-square linear displacement of $(2\,Dt)^{1/2}$ [26]. The fast lifetime of 7.9 μs measured from PNAM in toluene corresponds to 206 nm with the same diffusion coefficient of PtCP in toluene. Although the solvent conditions are the same as toluene, the lifetimes of the singlet oxygen molecules generated from the pure PtCP and PNAM are much different. The diffusion distance of 206 nm for the 7.9 μs is approximately similar to the pore diameter of 250 nm of the PNAM. The inner pore surface of PNAM is expected to be much covered by the hydroxyl groups that provide the efficient quenching for singlet oxygens. Therefore, it is suggested that 7.9 μs of the singlet oxygen lifetime is due to the collisional quenching of singlet oxygen to the hydroxyl groups on the surface of PNAM. [11]. Interestingly, the singlet oxygen life time from PNAM in aqueous solution is measured to be 2.8 μs (Figure 4(c)). It is the value that well correlates with the reported values of 2$\sim$4 μs which are the typical singlet oxygen lifetimes in aqueous solution [27]. When the same diffusion distance estimation is done, the lifetime of 2.8 μs from PNAM in aqueous solution corresponds to 94 nm (here, D equals to 1.57×10^{-9} m^2s^{-1} in aqueous solution). Since the estimated diffusion distance of 94 nm is much shorter than the pore diameter of PNAM, most singlet oxygens are expected to be more efficiently quenched by the nearby solvent water molecules.

Vesicular stomatitis virus is a very well-characterized lipid-enveloped virus which, together with its sensitivity for photodynamic treatment, makes it a suitable candidate for the study of photodynamic inactivation [28]. Therefore, in

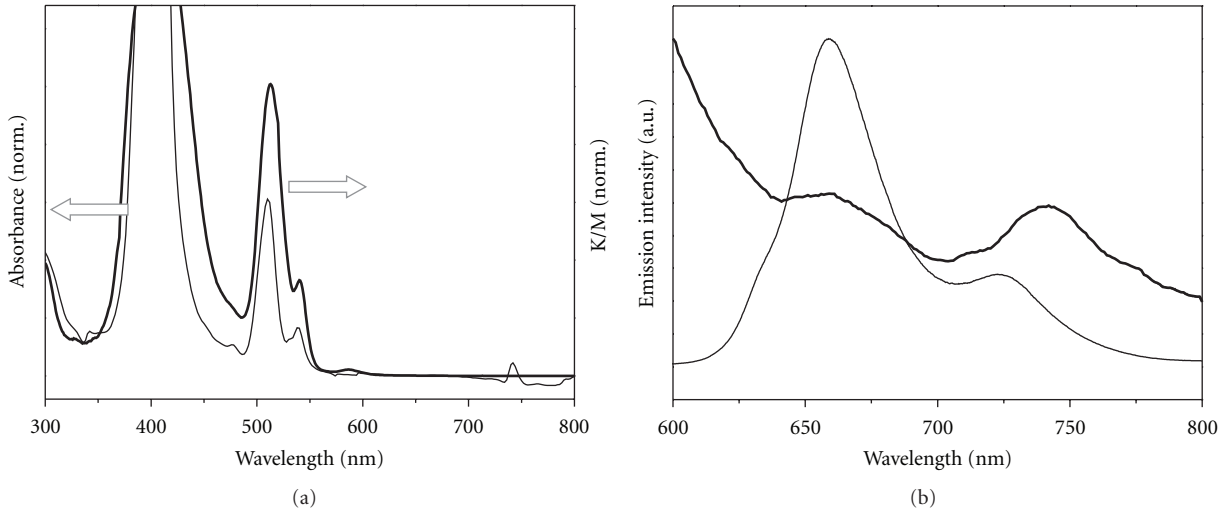

Figure 3: (a) Absorption and (b) phorescence spectra of the pure PtCP in toluene solution (thin solid line) and PNAM (thick solid line). The absorption spectrum of PNAM is obtained by applying the Kubelka-Munk function to the diffuse reflectance spectrum. The excitation wavelength was 510 nm for the emission spectra.

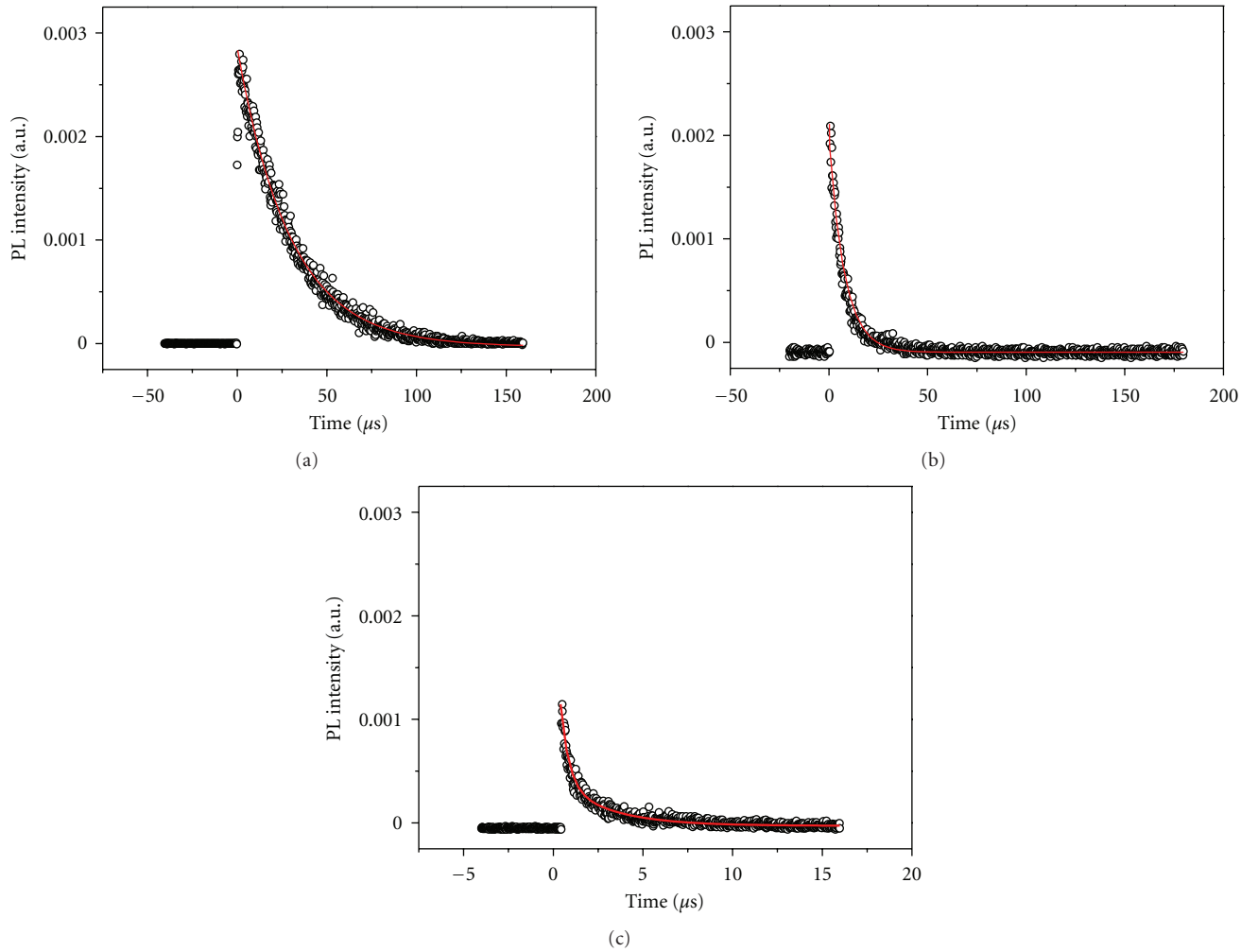

Figure 4: Phosphorescence decays of the singlet oxygens from (a) the pure PtCP in toluene, (b) PNAM with pore diameters of 250 nm in toluene, and (c) PNAM with pore diameters of 250 nm in aqueous solution at the detection wavelength of 1270 nm. The solid lines are the fitted lines with a single exponential decay.

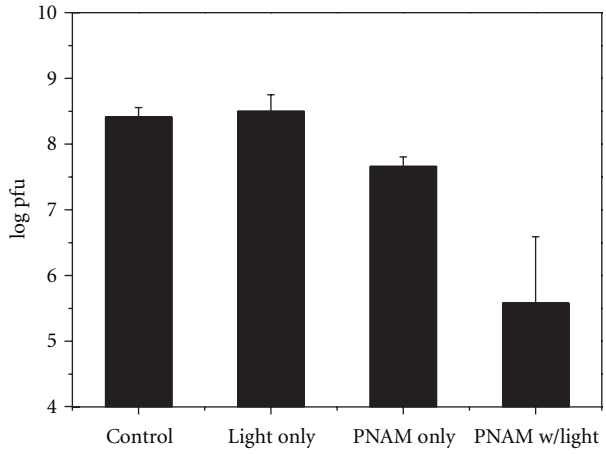

Figure 5: Plaques formed in A549 cells by the VSV treated with PNAM and light (5 mW). Extent of the VSV-induced PFU in A549: (control) normal level of PFU in A549 cells caused by VSV, (light only) virus treated with light only without PNAM, (PNAM only) virus treated with PNAM only without light, and (PNAM w/Light) virus treated with PNAM and light.

this study, the inactivation of VSV by the photo-irradiated PNAM was investigated to determine the PACT efficiency for the preliminary evaluation of the fabricated PNAM. As shown in Figure 5, the extent of the VSV-induced PFU in A549 cells was not changed by the light only factor. VSV (5×10^8 PFU/mL) caused the normal level of PFU in A549 cells (Figure 5 (control)). The same level of PFU in A549 cells as the control case was reproduced by the virus treated with light only without PNAM. The slightly decreased level of PFU in A549 cells was observed by the virus treated with PNAM without light (5×10^7 PFU/mL). Such a slightly low value of 5×10^7 PFU/mL is possibly expected due to the experimental condition of physical contact during stirring process of solution and also a residual room light effect. However, the virus treated with PNAM with light produced the PFU level of 5×10^5 PFU/mL in A549 cells, which is the significantly lower value than $5 \times 10^8 \sim 5 \times 10^7$ PFU/mL. Therefore, it clearly indicates that the fabricated PNAM in this study is an effective tool for PACT.

4. Conclusions

It has successfully been demonstrated that the singlet oxygen of highly oxidative species is generated from PNAM which is fabricated by the surface modification of NAM with organosilane agents, APTES, and the photosensitizer of PtCP. The singlet oxygen lifetimes depending on the pore diameter of PNAM and the solvent environment were also investigated to understand their dynamics in restricted condition that directly affects the efficiency of PACT. The photo-irradiated PNAM for the application of PACT was performed with the inactivation of VSV. The VSV was significantly inactivated by PNAM-PACT under 5 mW of light condition. Therefore, it suggests that the developed PNAM from this study has a high possibility to be utilized as a photodynamic antiviral system. Furthermore, based on the experimental results of the controlled singlet oxygen lifetimes by the pore diameter of the membrane, this ROS generating nanoporous membrane can be developed as the spatial distance selective photocatalytic membrane for biological and environmental hazards as well as selective photocatalytic reaction.

Acknowledgments

This study was supported by a grant of the Korea Healthcare Technology R&D Project, Ministry of Health & Family Affairs, Republic of Korea. (grant no. A085136). The authors are grateful to Prof. H. K. Kim for the generous support of PtCP and Dr. S. I. Oh for the help in the preparation of NAM.

References

[1] Y. Li, Y. Li, H. Liu et al., "Self-assembled monolayers of porphyrin-perylenetetracarboxylic diimide-[60] fullerene on indium tin oxide electrodes: enhancement of light harvesting in the visible light region," *Nanotechnology*, vol. 16, no. 9, pp. 1899–1904, 2005.

[2] K. Kalka, H. Merk, and H. Mukhtar, "Photodynamic therapy in dermatology," *Journal of the American Academy of Dermatology*, vol. 42, no. 3, pp. 389–416, 2000.

[3] R. Bonnetta, M. A. Krystevab, I. G. Lalovb, and S. V. Artarsky, "Water disinfection using photosensitizers immobilized on chitosan," *Water Research*, vol. 40, no. 6, pp. 1269–1275, 2006.

[4] L. Villén, F. Manjŏn, D. G. Fresnadillo, and G. Orellana, "Solar water disinfection by photocatalytic singlet oxygen production in heterogeneous medium," *Applied Catalysis B*, vol. 69, no. 1-2, pp. 1–9, 2006.

[5] C. J. Liu, S. G. Li, W. Q. Pang, and C. M. Che, "Ruthenium porphyrin encapsulated in modified mesoporous molecular sieve MCM-41 for alkene oxidation," *Chemical Communications*, no. 1, pp. 65–66, 1997.

[6] W. S. Chae, S. W. Lee, S. J. Im et al., "Hierarchically ordered CdS doped nanoporous membrane," *Chemical Communications*, vol. 10, no. 22, pp. 2554–2555, 2004.

[7] H. Masuda and M. Satoh, "Fabrication of gold nanodot array using anodic porous alumina as an evaporation mask," *Japanese Journal of Applied Physics*, vol. 35, no. 1, part 2, pp. L126–L129, 1996.

[8] A. M. M. Jani, J. Zhou, M. R. Nussio, D. Losie, J. G. Shapter, and N. H. Voelcker, "Pore spanning lipid bilayers on silanised nanoporous alumina membranes," in *Smart Materials V*, vol. 7267 of *Proceedings of SPIE*, pp. 0T01–0T10, Melbourne, Australia, December 2008.

[9] V. Szczepanski, I. Vlassiouk, and S. Smirnov, "Stability of silane modifiers on alumina nanoporous membranes," *Journal of Membrane Science*, vol. 281, no. 1-2, pp. 587–591, 2006.

[10] I. Vlassiouk, A. Krasnoslobodtsev, S. Smirnov, and M. Germann, "'Direct' detection and separation of DNA using nanoporous alumina filters," *Langmuir*, vol. 20, no. 23, pp. 9913–9915, 2004.

[11] K. K. Wang, M. S. Min, K. H. Choi et al., "Fabrication and photophysical properties of singlet oxygen generating nanoporous membrane," *Surface & Coatings Technology*, vol. 205, no. 15, pp. 3905–3908, 2011.

[12] J. McMurry, *Organic Chemistry*, Brooks/Cole, 5th edition, 2000.

[13] K. K. Wang, K. H. Choi, H. W. Shin et al., "Photophysics of a new photosensitizer with high quantum yield of singlet oxygen generation and its application to stereo-selective synthesis of (+)-deoxoartemisinin," *Chemical Physics Letters*, vol. 482, no. 1–3, pp. 81–86, 2009.

[14] J. H. Ha, S. Ko, C. H. Lee, W. Y. Lee, and Y. R. Kim, "Effect of core atom modification on photophysical properties and singlet oxygen generation efficiencies: tetraphenylporphyrin analogues core-modified by oxygen and/or sulfur," *Chemical Physics Letters*, vol. 349, no. 3-4, pp. 271–278, 2001.

[15] Y. J. Park, W. Y. Lee, B. S. Hahn, M. J. Hahn, J. K. Roh, and B. S. Kim, "The effective use of chlorophyll derivatives (CpD) photodynamic therapy of ascites tumors in mice," *Journal of Korean Cancer Association*, vol. 21, pp. 1–6, 1989.

[16] V. K. S. Hsiao, J. R. Waldeisen, Y. Zheng, P. F. Lloyd, T. J. Bunning, and T. J. Huang, "Aminopropyltriethoxysilane (APTES)-functionalized nanoporous polymeric gratings: fabrication and application in biosensing," *Journal of Materials Chemistry*, vol. 17, no. 46, pp. 4896–4901, 2007.

[17] K. Ishibashi, K. Tanaka, A. H. Iwata, K. Miyamoto, Y. Kimura, and M. Niwano, "In situ study of DNA attachment and hybridization at silicon surfaces by infrared absorption spectroscopy," *Japanese Journal of Applied Physics*, vol. 47, no. 4, pp. 3204–3208, 2008.

[18] K. H. Choi, K. K. Wang, S. I. Oh et al., "Singlet oxygen generating nanolayer coatings on NiTi alloy for photodynamic application," *Surface & Coatings Technology*, vol. 205, supplement 1, pp. S62–S67, 2010.

[19] D. L. Pavia, G. M. Lampman, and G. S. Kriz, *Introduction to Spectroscopy*, Brooks/Cole, 3rd edition, 2001.

[20] V. R. Rai and S. Agarwal, "Mechanism of self-catalytic atomic layer deposition of silicon dioxide using 3-aminopropyl triethoxysilane, water, and ozone," *Chemistry of Materials*, vol. 23, no. 9, pp. 2312–2316, 2011.

[21] J. Kim, J. Cho, P. M. Seidler, N. E. Kurland, and V. K. Yadavalli, "Investigations of chemical modifications of amino-terminated organic films on silicon substrates and controlled protein immobilization," *Langmuir*, vol. 26, no. 4, pp. 2599–2608, 2010.

[22] Y. H. Yu, C. C. M. Ma, S. M. Yuen et al., "Morphology, electrical, and rheological properties of silane-modified silver nanowire/polymer composites," *Macromolecular Materials and Engineering*, vol. 295, no. 11, pp. 1017–1024, 2010.

[23] P. Kubelka and F. Munk, "Ein beitrag zur optik der farbanstriche," *Zeitschrift fur Technische Physik*, vol. 12, pp. 593–601, 1931.

[24] B. T. Holland, C. Walkup, and A. Stein, "Encapsulation, stabilization, and catalytic properties of flexible metal porphyrin complexes in MCM-41 with minimal electronic perturbation by the environment," *The Journal of Physical Chemistry B*, vol. 102, no. 22, pp. 4301–4309, 1998.

[25] S. Subbiah and R. Mokaya, "Synthesis of transparent and ordered mesoporous silica monolithic films embedded with monomeric zinc phthalocyanine dye," *Chemical Communications*, vol. 9, no. 7, pp. 860–861, 2003.

[26] M. Okamoto, "Diffusion processes involved in the exothermic triplet-triplet energy transfer in n-hexane at high pressure: evaluation of diffusion coefficients of benzophenone, triphenylene and naphthalene," *Journal of Photochemistry and Photobiology A*, vol. 162, no. 1, pp. 17–22, 2004.

[27] K. Lang, J. Mosinger, and D. M. Wagnerova, "Photophysical properties of porphyrinoid sensitizers non-covalently bound to host molecules; models for photodynamic therapy," *Coordination Chemistry Reviews*, vol. 248, no. 3-4, pp. 321–350, 2004.

[28] J. Parker, P. B. Ahrens, and H. Ankel, "Antiviral effect of cyclopentenone prostaglandins on vesicular stomatitis virus replication," *Antiviral Research*, vol. 26, no. 1, pp. 83–96, 1995.